Experimental Testing of the Polymer–Filler Gel Formation Theory. II.

L. KARÁSEK,* B. MEISSNER

Prague Institute of Chemical Technology, Polymer Department, 16628 Prague 6, Czech Republic

Received 4 June 1997; accepted 3 September 1997

ABSTRACT: In Part I of the present article predictions of the polymer–filler gel formation theory were tested experimentally using fine-particle silica in natural rubber (NR) and in styrene–butadiene rubber (SBR). Part II brings a more detailed experiment–theory comparison using carbon blacks differing in specific surface area and structure, graphitized blacks, fume silica, and surface-modified (hydrophobized) fume silica. In the region of low and medium filler concentration c, the c-dependence of the fraction G of polymer in polymer–filler gel, of the fraction B of total filler-bound polymer, of the fraction w_{disp} of solvent-dispersed filler particles were found to be correctly predicted by the theory. The effect of filler characteristics and of the method of its incorporation into the polymer on the values of the adjustable parameters of the theory (filler surface adsorptivity, D, and filler particles connectivity, f) was determined and is discussed. In the region of very high c increasing positive deviations of D from the low-c behavior were observed and an explanation for this effect is proposed. © 1998 John Wiley & Sons, Inc. J Appl Polym Sci 69: 95–107, 1998

Key words: adsorption; polymer–filler interaction; filler-induced gelation of polymers; carbon black; polyfunctional crosslinks

INTRODUCTION

Part I[1] reported experimental data on the filler-induced insolubilization of polymer and on the formation of a gel-like structure in compounds of natural rubber (NR) and styrene–butadiene rubber (SBR) containing fine-particle silica (Aerosil OX-50). The following characteristics were determined: B, fraction of bound rubber, given by the total amount of polymer adsorbed from bulk on filler particles; G, fraction of gel polymer, given by the amount of polymer that forms a macroscopic three-dimensional gel-like structure with some ($G < B$) or all ($G = B$) filler particles present in the compound; w_{disp}, fraction of filler dispersed by the solvent. The dependences of G, B, and w_{disp}, on filler concentration c (filler-to-polymer mass ratio in the compound) were then compared with the predictions of the polymer–filler gel formation (PFGF) theory,[2] which is based on a model of filler particles acting as a polyfunctional crosslinking agent for polymer chains:

$$G = 1 - \int_0^\infty w(y)\exp[-q_{cr}y(1 - S^{f-1})]dy \quad (1a)$$

$$B = 1 - \int_0^\infty w(y)\exp(-q_{cr}y)dy \quad (1b)$$

$$w_{\text{disp}} = S^f$$

$$q_{cr} = \frac{cPDM_o}{N_A} \quad (1c)$$

Correspondence to: B. Meissner, Institute of Macromolecular Chemistry, Academy of Sciences of the Czech Republic, 16206 Prague 6, Czech Republic.

* *Present address:* Kordárna a.s., 69674 Velká nad Veličkou 890, Czech Republic.

Contract grant sponsor: Grant Agency of the Czech Republic; contract grant number: 203/94/0915.

Journal of Applied Polymer Science, Vol. 69, 95–107 (1998)
 CCC 0021-8995/98/010095-13

Here, y is the number of crosslinkable structural units in a primary polymer chain, $w(y)dy$ is the mass fraction of chains having y in the range between y and $y + dy$, q_{cr} is the fraction of crosslinked (filler adsorbed) structural units, S is the fraction of sol ($S + G = 1$), M_o is the molar mass of the polymer structural unit, N_A is the Avogadro constant, D is the number of reactive sites per unit of filler surface area, and f is the number of crosslinked structural units per crosslink (the filler particle functionality).

More detailed description of the PFGF theory and of the experimental measurements is given in Part 1. The measure of agreement between the predicted and experimentally determined dependences of B on c and between the theoretical and experimental G vs. B and w_{disp} vs. B correlations was found to be good to very good. The two adjustable parameters of the polymer–filler gel formation theory ($D = 1/A_o$, f) were determined and found to assume reasonable values. A_o is identical with the quantity defined before in the bound rubber theory,[3] and represents the filler surface area per one reactive site. Both D and A_o are simple characteristics of the filler activity for polymer bonding. The values of D were found[1,3–5] to be of the order of 10^{16} m^{-2}. The functionality, f, of the crosslinking particles is a measure of their connectivity and its values were found to lie in the 10–30 range for the Aerosil OX 50–NR and SBR systems and also for the carbon black N765–SBR system.[5] Using simplifying assumptions, the size of the (hypothetical) crosslinking particle was calculated from the data and found to be smaller than that of the actual filler particles (aggregates).

This article reports further experimental data obtained on various polymer–filler systems. The effect of several factors (concentration and type of filler, mixing conditions, molar mass distribution of the polymer) has been studied in an effort to elucidate the nature of polymer–filler interaction in more detail.

EXPERIMENTAL

Materials

White crepe grade of natural rubber (NR) was cold milled to obtain samples of medium (NR-A) and high (NR-B) degree of mastication breakdown. These were then used for compound preparation. Data characterizing their solution viscosity and molar mass distribution (GPC) are given in Table I.

Styrene–butadiene rubber (SBR) (Kralex 1502 produced by the Kauěuk factory, Kralupy n.Vl., Czech Republic) was given a mild cold mill breakdown (5 min) before compound preparation. Results of viscosity and GPC measurements are given in Table I.

Seven types of carbon black differing in specific surface area, structure, and surface activity and two silica fillers were used. Their properties are given in Table II.

Preparation of Polymer–Filler Compounds

Method A

Most polymer–filler compounds with varying filler concentration were prepared using a procedure that is hoped to minimize the molar mass changes of polymer during filler incorporation. The required amount of polymer was cut into small pieces and dissolved in benzene. Filler was added to the solution with stirring and the solvent was let to evaporate slowly. The film of polymer and filler that had arisen after solvent evaporation was then processed on a two-roll mill, care being taken to ensure a good dispersion of the filler in the elastomer.

Method B

One of the series (SBR–N330 compounds) was prepared as follows: compound with the highest carbon black concentration $c = 0.5$ was prepared in a laboratory internal mixer and the compounds with lower concentrations were then obtained by diluting it with polymer on a two-roll mill.

Method C

The NR-Aerosil OX50 compounds were prepared using Brabender Plastograph in a manner already described.[1]

After filler incorporation all compounds were sheeted-out on a two-roll mill and compression molded at 145°C for 1 h to obtain specimens of ca. 1 mm thickness. The filler concentration c in the respective compounds was checked using thermogravimetric measurements.

Gel Content Determination

The procedure was similar to but not identical with that used previously.[1] Small samples of

Table I Characterstics of Polymer Samples

Rubber Sample	NR-A Medium Breakdown	NR-B Highly Masticated	SBR 5-Min Cold Milled
$[\eta]$ (toluene) dL/g	2.23	1.15	1.89
$\bar{M}_v$ kg/mol	294[a]	110[a]	170[b]
GPC			
$\bar{M}_w$ kg/mol	325	140	236
$\bar{M}_u/\bar{M}_n$	2.26	1.79	3.35
$\bar{M}_z/\bar{M}_w$	1.77	1.71	2.57

[a] Carter, Scott, Magat[6]: $[\eta] = 5.02 \times 10^{-4} M_r^{0.667}$.
[b] Homma, Fujita[1,7]: $[\eta] = 5.58 \times 10^{-4} M_r^{0.675}$.
M_r = relative molecular mass.

known mass m were placed into weighed pouches (bags) made of polyamide monofilament fabric with a mesh size of several tenths of a millimeter. The sample mass $m = m_p + m_f$, where m_p is the mass of polymer, m_f the mass of filler; $c = m_f/m_p$ is the filler concentration. The nongel part of the sample (i.e., solvent-dispersed filler particles of mass m_{f2} with polymer chains of mass m_{p2} adsorbed on them + soluble filler-unbound polymer chains of mass m_{p1}) was removed from the sample by toluene extraction. This was assisted by moving the pouch slowly up and down from time to time. The solvent was changed several times during 5 days. For carbon black compounds the solvent dispersed filler is clearly visible. At low filler concentrations (below and slightly above the gel point) the solvent-dispersed filler–polymer particles are small, show no signs of interconnection, and color the first portions of the solvent black. With increasing filler concentration in the compound the size distribution of solvent-dispersed filler–polymer particles widenes. Apart from fine-size particles, there are larger and larger filler–polymer structures visible, which obviously consist of several filler particles (aggregates) connected through polymer chains and swollen by the solvent. Their size is smaller than the mesh size of the fabric. After a sufficient time of extraction the newly added solvent remaines clear and containes no black particles. This indicates approaching the end of the extraction. The part of the system remaining in the pouch then consists of swollen filler–polymer particles that are larger than the mesh size. Even in the deswollen state the volume of such filler–polymer particles is at least several orders of magnitude larger than that of the initial components—polymer chains and/or carbon black particles (aggregates). From the

Table II Properties of Fillers

Filler	Source	Description	P m^2/g
Aerosil OX50	Degussa, Germany	fume silica	50
HDKH2000	Wacker, Germany	hydrophobized fume silica	170
Nigros I (ISAF N220)	Deza, Cz. Rep.	furnace black	86.3
Nigros K (HAF N330)	Deza, Cz. Rep.	furnace black	66.4
Nigros F (FEF N550)	Deza, Cz. Rep.	furnace black	45.2
Durex O	Degussa, Germany	lamp black	20.4
Sevacarb MT (N990)	Phillips, USA	thermal black	7.5
gN330	Degussa, Germany	graphitized N330 black	82
Ensaco 50E	MMM Carbon	graphitized, very high structure	43.5

Dibutyl phthalate absorption (mL/100 g) of carbon blacks: MT 38, Ensaco 50E 293, Nigros I, K, F around 100. DBPA 24M4 of Ensaco 50E 137 mL/100 g.

The P (CTAB), DBPA-values of Nigros I, Nigros K, Nigros F (declared as ISAF N220, HAF N330, FEF N550, respectively) and of lamp black were supplied by the Institute of Rubber Technology and Testing, Zlin (Czech Republic). The P, DBPA-values of the remaining blacks are those given by the producers. The furnace blacks Nigros I, Nigros K, Nigros F of the Deza Co. are now out of production.

practical point of view such a large filler–polymer particle may be regarded as an "infinite" macroscopic three-dimensional structure, i.e., gel. The filler–polymer particles smaller than the mesh size and removed from the pouch by the solvent are then arbitrarily considered as belonging to the sol because the order of their magnitude does not differ sufficiently from that of the filler particles (aggregates). The thoroughly extracted gel remaining in the pouch is dried, weighed, and after subtracting the mass of the dried pouch fabric the mass of the polymer–filler gel ($m_{p3} + m_{f3}$) is obtained (m_{p3} is the mass of gel polymer, m_{f3} the mass of filler in the polymer–filler gel).

At a still larger filler concentration in the compound, c, the fraction of solvent-dispersed fine-size filler–polymer particles decreases to zero, and only the somewhat larger filler–polymer structures that do not color the solvent are seen in the solvent in the early stages of extraction. Finally, above the filler concentration for coherent gel formation, c_{coh}, no visible filler–polymer particles are removed from the pouch because all filler particles have become incorporated into the polymer–filler gel ($m_{f3} = m_f$). The mass of the polymer–filler gel can then be determined without using any fabric filter because only polymer is being extracted from the compound and the gel is coherent.

The mass ($m_{p3} + m_{f3}$) of the polymer–filler gel can be expressed relatively with respect to the mass of polymer or with respect to the mass of filler in the sample:

$$R_p = \frac{m_{p3} + m_{f3}}{m_p}; \quad R_f = \frac{m_{p3} + m_{f3}}{m_f} \qquad (2)$$

The composition of the extracted polymer–filler gel was determined using a thermogravimetric analysis: in the stream of nitrogen at high temperatures the polymer is degraded and distilled off while carbon black remains unchanged. This gives the polymer–filler mass ratio in the gel, $R_3 = m_{p3}/m_{f3}$. A relative quantity $R_{f3} = R_3 + 1$ expresses the polymer–filler gel composition in a way more comparable to R_p, R_f:

$$R_{f3} = \frac{m_{p3} + m_{f3}}{m_{f3}} \qquad (3)$$

R_{f3}, the ratio of mass of polymer–filler gel to mass of filler in the gel, is generally higher than R_f, but at higher filler concentrations $m_{f3} \to m_f$ and the two quantites become identical.

Molar Mass Distribution

Molar mass distribution of the (masticated) samples of NR and SBR was obtained by GPC using tetrahydrofurane as a mobile phase, polystyrene standards, and the concept of universal calibration. The molar mass distribution curve of SBR (Kralex 1502 milled 5 min) is shown in Figure 11.

RESULTS AND DISCUSSION

Determination of D, f from R_p, R_f

At filler concentrations that are higher than the concentration for coherent gel formation, c_{coh}, the experimental values of $G\ (= B)$ are obtained easily from weighing data. In the concentration region between the gel-point concentration, c_{gp} and c_{coh}, they can be determined by combining the information obtained by weighing (R_p) and by thermogravimetry (R_3):

$$G(= m_{p3}/m_p) = R_p R_3/(R_3 + 1) \qquad (4)$$

We have observed, however, that this way of data processing may contribute to the scatter of calculated G-values. When R_3-values are low, it may lead to a systematic shift. Determination of mass by weighing is intrinsically more reliable than thermogravimetric measurement of the polymer–filler mass ratio in the gel and the R_p and R_f-values obtained by weighing are subject to less uncertainty and scatter than R_3. It is, therefore, advantageous to compare them with the predictions of the PFGF theory directly. For this purpose eq. (1) has been used to obtain the theoretical values of R_p and R_f. Using definitions $G = m_{p3}/m_p$, $w_{\text{disp}} = m_{f2}/m_f$, $m_{f3}/m_f = 1 - w_{\text{disp}}$ the following result is obtained:

$$R_p = G + (1 - (1 - G)^f)c;$$
$$R_f = (G/c) + (1 - (1 - G)^f) \qquad (5)$$

where $(1 - G)^f$ is equal to the fraction w_{disp} of solvent-dispersed filler particles [eq. (1c)].

An example of the concentration dependences of the ratios R_p and R_f, determined experimentally for the SBR–N330 series (mixing method B)

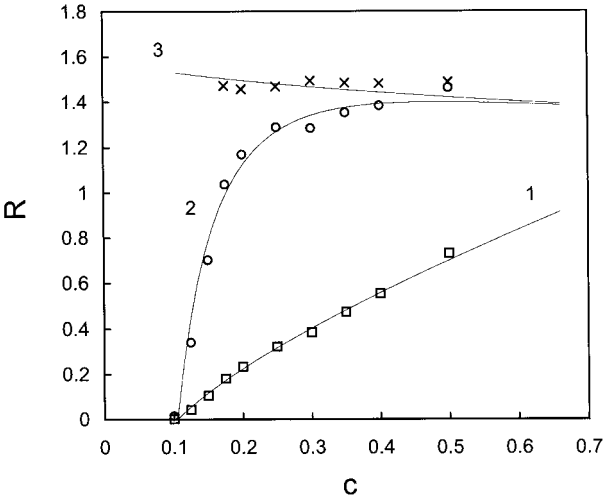

Figure 1 Dependence of R_p (curve 1), R_f (curve 2), R_{f3} (curve 3) on filler-to-polymer ratio c in the SBR–HAF black compound (mixing method B). Points: experimental (R_p, R_f from weighing data, R_{f3} from thermogravimetry). Curves 1, 2, and 3, respectively, are drawn using eqs. (1a), (5), and (6); parameter values given in Table III and molar mass distribution of polymer determined by GPC.

is shown in Figure 1. The R_p vs. c dependence is almost linear, whereas the R_f vs. c dependence has a hyperbolic-type shape. The R_f-values increase rapidly above the gel point while assuming an almost constant value at higher filler concentrations. The theoretical curves were calculated from the eqs. (1a) and (5). The experimentally determined molar mass distribution $w(\log M)\, d \log M$ was inserted and the integration (summation) was done numerically for suitably chosen values of the adjustable parameters D and f. The theoretical curves were fitted to the data in such a way as to satisfy the R_p vs. c and R_f vs. c dependences simultaneously. This adds to the reliability of the D and f estimates. For the given system the following parameter values were determined: $D = 2.16 \times 10^{16}$ m^{-2}, $f = 18$. The point belonging to the highest filler concentration was given a somewhat smaller statistical weight because the preparation of the compound in question differed slightly from that of the other ones (there was no diluting step with unfilled polymer in this case). One more example of R_p vs. c and R_f vs. c dependences and their comparison with theoretical curves is shown in Figure 2 for the SBR–HDK H2000 system.

All our experimental concentration dependences of R_p and R_f obtained for the individual polymer–filler series (in the concentration range from 0 to c_{max}) were processed in the manner described. The resulting values of the adjustable parameters D and f, are summarized in Tables III and IV, together with the highest concentration c_{max}, which was taken into account in the calculation (for SBR–N330 method B and for the NR-A and NR-B series, c_{max} was the highest concentration that was available). The filler concentrations c_{gp} in the gel point are also given in Tables III and IV. They were determined from the intersection of the theoretical curves with the concentration axis.

In Figure 1 the results of thermogravimetry, R_{f3}, are also plotted and compared with the theoretical values of R_{f3}:

$$R_{f3} = \frac{G}{(1 - (1 - G)^f)c} + 1 \qquad (6)$$

The theoretical curve 3 was calculated using eqs. (1a) and (6) and the D and f-values obtained above. The deviations of the experimental points from the theoretical curve may be regarded as small to insignificant in this case. The R_{f3}-values that are plotted in Figure 2 for the modified silica–SBR system were determined from the mass of the residue after burning the extracted sample in a laboratory furnace (see Part I). The scatter

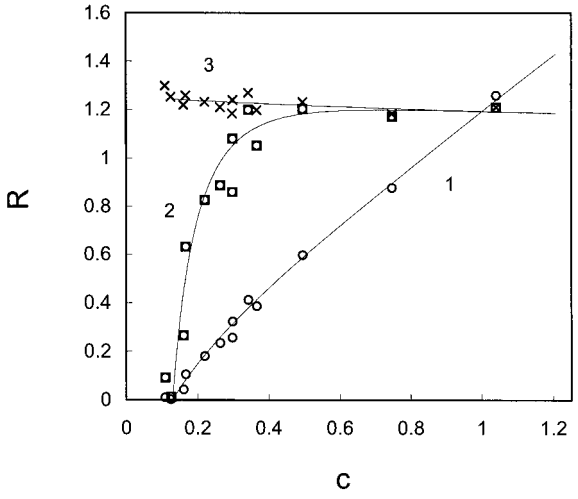

Figure 2 Dependence of R_p (curve 1), R_f (curve 2), R_{f3} (curve 3) on filler-to-polymer ratio c in the SBR–HDK H2000 compound (mixing method A). Points: experimental (R_p, R_f from weighing data, R_{f3} from the ash residue). Curves 1, 2 and 3, respectively, are drawn using eqs. (1a), (5), and (6); parameter values given in Table III and molar mass distribution of polymer determined by GPC.

Table III Values of c_{gp}, D, f, A_0 Obtained from R_p vs. c, R_f vs. c Dependences

		SBR				
Filler	Mixing Method	$c_{max} \times 10^2$	$c_{gp} \times 10^2$	D (m^{-2}) $\times 10^{-16}$	f	A_0 nm^2
N220	A	90	5.4	1.60	35	62.5
N330	A	90	7.2	1.48	37	67.6
N330	B	40 (50)	10.5	2.16	18	46.3
N550	A	90 (110)	8.4	1.98	35	50.5
La	A	80	18.6	1.57	44	63.8
MT	A	180	57.0	1.53	40	65.1
gN330	A	120	6.9	0.41	110	243
Ensaco 50E	A	80	9.0	0.66	100	152
HDK H2000	A	105	12.9	0.38	32	265

of the data is somewhat higher than in Figure 1, but the expected trend is visible.

Bound rubber or polymer–filler gel measurements described in the literature are sometimes done under conditions that are not sufficient for a thorough extraction of the filler-unbound polymer. An experiment was undertaken here to explore such effects. The solvent was not replaced by a fresh one during the 5 days of extraction, and the sample was kept static, without any movement. The result is shown in Figure 3. The filler concentration in the gel point, c_{gp}, decreased from ca. 0.1 to ca. 0.05 and, as a result, the estimated value of f increased substantially (from 18 to 38). Results of thermogravimetric measurements were seriously affected and the R_3 values at low c were significantly higher than those in the previous experiment. This demonstrates that incomplete removal of filler-unbound polymer (and/or of solvent-dispersible filler particles) may lead to erroneous results and incorrect conclusions.

Calculation of G, w_{disp}, and B, and Comparison with Theory

Although in the concentration range between c_{gp} and c_{coh} the G-values cannot be calculated from weighing data alone (i.e., from R_p or R_f), they can be derived from the latter experimental information if one combines it with the knowledge of the parameter f. As shown above, f can be obtained from the comparison of the experimental R_p vs. c and R_f vs. c dependences with theory. Once f is known, the required G-values can be calculated from each experimental R_p-value by solving eq. (5).

In this way the G-values in the range of c between c_{gp} and c_{coh} were obtained for all polymer–filler series. In Figure 4 the dependences of G on filler concentration are plotted for the three furnace blacks, lamp black, and MT black in SBR. The G vs. c dependences are shown for the two graphitized blacks in Figure 5.

Description of data by theoretical curves may be characterized as satisfactory or even convincing. Most polymer–filler systems conform to the theoretical predictions up to concentrations c of 0.9–1.2, the SBR–MT black system up to 2.

In Figure 6 the G-values of NR-A and NR-B compounds containing Aerosil OX 50 are A:index plotted vs. the crosslinking index $\gamma = cPD\overline{M}_w/N_A$ (N_A is the Avogadro constant). The two polymers NR-A and NR-B, have slightly different molar mass distributions and, therefore, the theoretical curves are not identical and diverge slightly at higher c. The concentration of filler in the gel point, c_{gp}, increases with decreasing molar mass

Table IV Values of c_{gp}, D, f, A_0 Obtained from R_p, R_f vs. c Dependences

			NR				
Polymer	Filler	Mixing method	$c_{max} \times 10^2$	$c_{gp} \times 10^2$	D (m^{-2}) $\times 10^{-16}$	f	A_0 nm^2
NR-A	Aerosil OX50	C	25	3.9	5.0	20	20.0
NR-B	Aerosil OX50	C	28	9.5	4.8	20	20.8

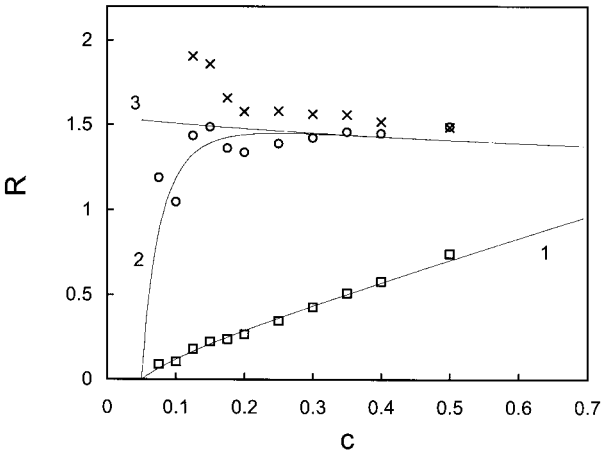

Figure 3 Dependence of R_p (curve 1), R_f (curve 2), R_{f3} (curve 3) on filler-to-polymer ratio c in the SBR–HAF black compound (mixing method B). Extraction without changing the solvent. Points: experimental (R_p, R_f from weighing data, R_{f3} from thermogravimetry). Curves 1, 2, and 3, respectively, are drawn using eqs. (1a), (5), and (6); parameter values $D = 2.08 \times 10^{16}$ m^{-2}, $f = 38$ and the GPC molar mass distribution data of polymer.

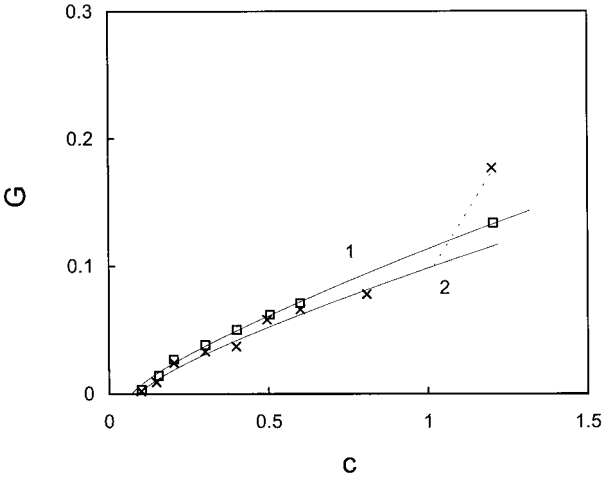

Figure 5 Dependence of the gel fraction G on filler-to-polymer ratio c in SBR-graphitized carbon black compounds. Experimental points calculated from weighing data using eq. (5). Theoretical curves drawn using eq. (1a); parameter values given in Table III and the GPC molar mass distribution data. Dependences: 1—graphitized N330, 2—Ensaco E50.

of the polymer (Table IV), and the same holds true for the concentration of filler for coherent gel formation, c_{coh}. On the other hand, the bound rubber fraction at c_{coh} is practically independent of the molar mass of the polymer. Consequently, the quantity $B/c_{coh}P$ (denoted as specific bound rubber for coherent gel formation by Wolff, Wang, and Tan[8]) is highly dependent on the molar mass of polymer. This should be taken into account when trying to use $B/c_{coh}P$ as a measure of the specific surface activity of filler.[8]

The experimental values of w_{disp} were calcu-

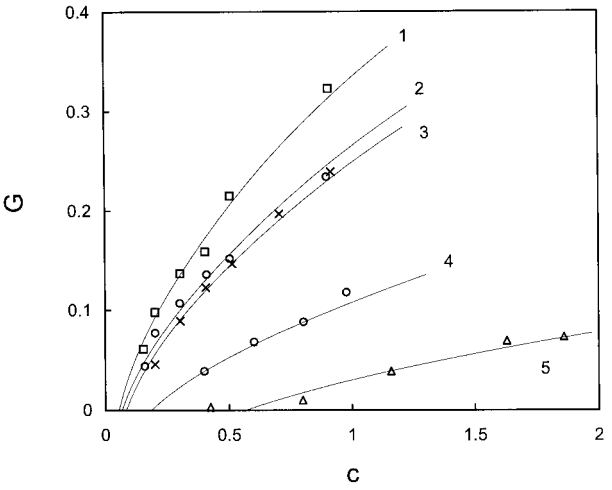

Figure 4 Dependence of the gel fraction G on filler-to-polymer ratio c in SBR–carbon black compounds. Experimental points calculated from weighing data using eq. (5). Theoretical curves drawn using eq. (1a); parameter values given in Table III and the GPC molar mass distribution data. Dependences: 1—ISAF, 2—HAF, 3—FEF, 4—lamp black, 5—MT black.

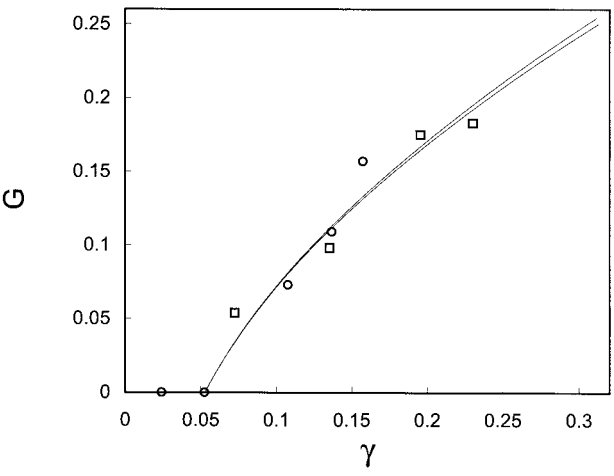

Figure 6 Dependence of the gel fraction G on the crosslinking index $\gamma = cPD\overline{M}_w/N_A$ in NR–Aerosil OX50 compounds. Variables: c, $\overline{M}_w$, polydispersity. Experimental points calculated from weighing data using eq. (5). Theoretical curves drawn using eq. (1a), GPC molar mass distribution data and parameter values given in Table IV. Squares: NR-A, circles: NR-B.

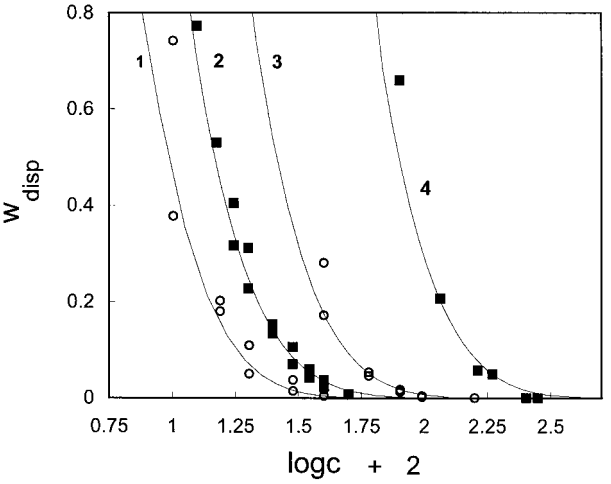

Figure 7 Dependence of the fraction w_{disp} of solvent-dispersed filler particles on the logarithm of filler-to-polymer ratio c in SBR–carbon black compounds. Experimental points calculated from weighing and thermogravimetric data using eq. (7). Curves are drawn using eqs. (1a) and (1c), and parameter values given in Table III. Dependences: 1—graphitized N330, 2—HAF, 3—lamp black, 4—MT black; 1, 3, 4—mixing method A, 2—mixing method B.

lated by combining the weighing and thermogravimetric data:

$$w_{\text{disp}} = 1 - \frac{R_f}{R_3 + 1} \tag{7}$$

In Figure 7, w_{disp} is plotted vs. log c for four polymer–filler series. The location of the theoretical curves (which were calculated using the D and f-values given in Table III) in the log c axis is determined by c_{gp}, which in turn is inversely proportional to the product $(f - 1)PD\overline{M}_w$ [eq. (10) in Part I]. The scatter of w_{disp} values is rather high but the general agreement with the predictions of the theory is good.

Above c_{coh} the fraction of total filler-bound polymer B is obtained easily from weighing measurements. Below c_{coh} the experimental determination of total mass of polymer $(m_{p2} + m_{p3})$ adsorbed on all filler particles $(m_{f2} + m_{f3})$ is not without difficulties. It requires thorough extraction of all components of the system, including solvent-dispersed filler particles. Repeated washing and centrifugation is necessary. In an attempt to obtain estimates of B in a less complicated way we have done a theoretical analysis of the predictions of the PFGF theory regarding the polymer–filler ratio in the gel (m_{p3}/m_{f3}) and in the sol (m_{p2}/m_{f2}). One of the results is shown in Figure 8. It is apparent that just above gel point the quantity B/c $[= (m_{p2} + m_{p3})/(m_{f2} + m_{f3})]$ does not differ very much from R_3 $(= m_{p3}/m_{f3})$, and with increasing c the difference disappears. It is interesting to see that the difference $[(B/c) - R_3]$ may be positive or negative, depending on the shape of the molar mass distribution of the polymer. The latter difference, however, is small and a satisfactory estimate of B can be calculated using a simple relation

$$B \approx cR_3$$

where $R_3 = m_{p3}/m_{f3}$ may be obtained either from thermogravimetry or by combining weighing data with information on f (see above). In the latter case, i.e., after f has been obtained by curve fitting and the experimental G-values have been calculated from R_p using eq.(5), an estimate of the

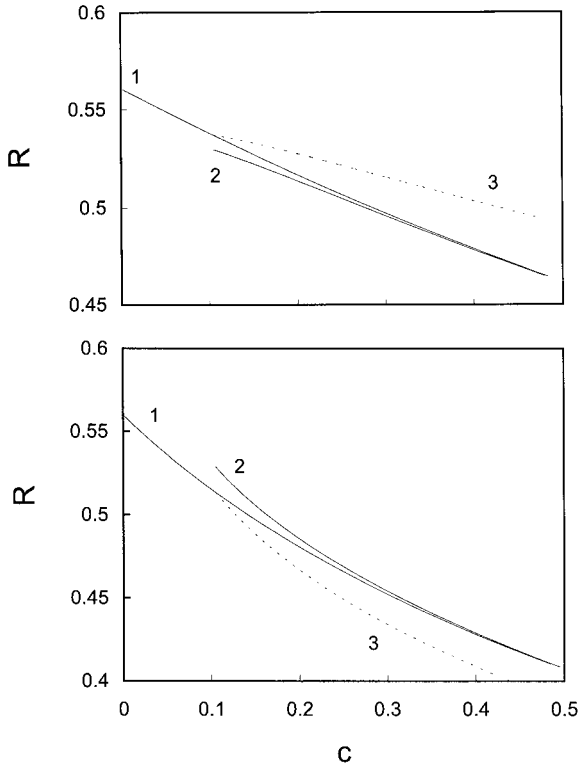

Figure 8 Theoretical dependences of R on c calculated using eqs. (1a) and (1b), and parameter values $D = 2.16 \times 10^{16}\ \text{m}^{-2}$, $f = 18$, $\overline{M}_w = 236$ kg/mol. Curves: 1—$R = B/c = (m_{p2} + m_{p3})/(m_{f2} + m_{f3})$, 2—$R = m_{p3}/m_{f3}$, 3—$R = m_{p2}/m_{f2}$. Top: most probable distribution. Bottom: logarithmic normal distribution $(\overline{M}_w/\overline{M}_n = 3.35)$.

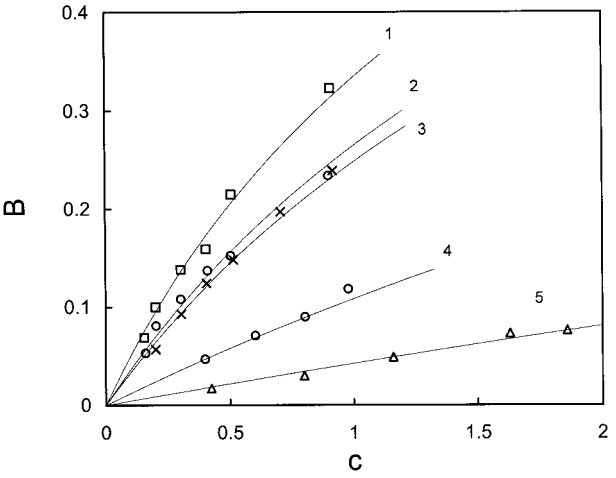

Figure 9 Dependence of the bound rubber fraction B on filler-to-polymer ratio c in SBR–carbon black compounds. Experimental points calculated from weighing data using eq. (8). Theoretical curves drawn using eq. (1b); parameter values given in Table III and the GPC molar mass distribution data. Dependences: 1—ISAF, 2—HAF, 3—FEF, 4—lamp black, 5—MT black.

bound rubber fraction is obtained from eq. (8) with an error of less than ca. 5%:

$$B \approx \frac{G}{1 - (1 - G)^f} \tag{8}$$

The concentration dependence of the bound rubber fraction for the five ungraphitized carbon blacks is shown in Figure 9.

Effect of Type of Filler and of Mixing Conditions on *D* and *f*

The following conclusions can be drawn from the D and f-values obtained and given in Tables III and IV: (1) the filler surface activity for bound rubber formation, D, is surprisingly little sensitive to the specific surface area of ungraphitized carbon blacks when the mixing method A is used (D ca. 1.5–1.6 (10^{16} m^{-2}), the only exception being the somewhat higher value of D found for Nigros K (N550 black). This finding is in agreement with our recent analysis[5] of published data[8] where the D-parameter obtained for the SBR–N550 system was also higher than that for the SBR–N220 and SBR–N330 systems. A significant increasing correlation of D with the difference between the dibutylphtalate absorption DBPA and the crushed dibutylphtalate absorption DBP 24M4 was found to exist for a group of 16 commercial rubber-grade blacks.[5] The effect was ascribed to the filler aggregates breakdown on mixing of higher structure blacks, which leads to a new active surface formation for polymer-to-filler bonding.[9]

The values of D and f recently obtained for the BR-ISAF black system[10] are similar to those found above for the SBR–ISAF black system. This suggests that the polymer–filler interaction leading to gelation and bound rubber formation is not significantly altered by the presence of 25% of styrene in the butadiene–styrene copolymer. (2) Graphitization of the high surface area, medium structure N330 black leads to a reduction of D by a factor of approximately 3.5. The graphitized very high structure lower surface area carbon black Ensaco 50E has a higher D than the graphitized N330. Obviously, the carbon black structure affects D in a similar way both in the group of ungraphitized and graphitized blacks. (3) The D-value of surface-modified (hydrophobized) fume silica in SBR (mixing method A) is similar to that of graphitized N330. It is smaller than that of unmodified fume silica (Aerosil OX50) by a factor of approx. 8. However, the latter filler was incorporated into SBR using a different mixing method.[1] (4) Mixing method B includes a hot step in the mixer and leads to a higher D-value and a lower f-value for N330 in SBR than the "cold" mixing method A. (5) Use of the "cold" mixing method A for the five ungraphitized carbon blacks leads to similar values of functionality f ($\approx$ 35 to 45), while the "hot" mixing method B used for the N330–SBR system gives a lower f (=18). Graphitization of carbon blacks leads to a decreased surface activity D but to a significantly increased particle connectivity f (ca. three times).

These observations may be tentatively explained using the concept of multiple segment adsorption of the same polymer chain on the same filler particle (aggregate).[1] Such an effect represents a deviation from the theory of random crosslinking. The latter assumes that crosslinking is exclusively intermolecular, i.e., a polymer chain after having reacted through one of its segments (structural units) at a crosslinking site belonging to one filler particle will react next time through another of its segments at a crosslinking site belonging to a different filler particle (aggregate). The chain is not allowed to form closed loops such as those resulting from multiple adsorption of a given polymer chain on the same filler particle (aggregate).

With no loops formation the functionality of a

filler particle (aggregate) having total surface area V_p and surface area per adsorption point A_o would be simply given by $f = V_p/A_o$. For instance, theoretical functionality of a primary particle of graphitized N330 with a diameter of $d \approx 30$ nm and $A_o = 243$ nm^2 (Table III) would be $\pi d^2/A_o = 11.6$. Theoretical functionality of an aggregate (which typically consists of 40–50 primary particles) would be ca. 500. The latter value is four to five times larger than the experimental functionality 110 obtained from the R_p vs. c dependence. This result may be perhaps regarded as a satisfactory order-of-magnitude agreement. For ungraphitized blacks, however, the ratio of theoretical and experimental f would be much larger.

If only a certain fraction β of adsorbed polymer segments (structural units) conforms to the theoretical requirement of no loop formation, then the filler functionality will be decreased to

$$f = \beta V_p/A_0 = \beta V_p D.$$

Let us analyze possible factors that might affect β. Adsorption of polymer segments on the filler surface takes place (a) during mixing, i.e., under dynamic conditions that may differ in temperature and level of shear stress; or (b) after mixing, in the finished compound under static conditions, at different temperatures. The first step is a certain sort of dynamic vulcanization where the rate and extent of segment adsorption (measured as B) will increase with temperature while polymer–filler gel-like structures of a larger size may be expected to be destroyed by mechanical shearing. One can imagine an extreme case where a substantial amount of polymer has been adsorbed on a fine-particle filler (say, $B = 0.3$) without having formed any gel at all: due to the shearing action a given chain did not succeed to adsorb on two (or more) different filler particles (aggregates), it formed two (or more) connections with the same particle (aggregate). In such a case β of the first step, i.e., β_1, would be zero. The second step proceeds under static conditions and is more favorable for the formation of three-dimensional structures. At the extreme, β corresponding to the second step (i.e., β_2) could approach 1, but more probably it is smaller then 1. The expression for f can be formally written as composed of two parts:

$$f = \beta_1 D_1 V_p + \beta_2 (D - D_1) V_p$$
$$= D V_p [\beta_1 D_r + \beta_2 (1 - D_r)]$$

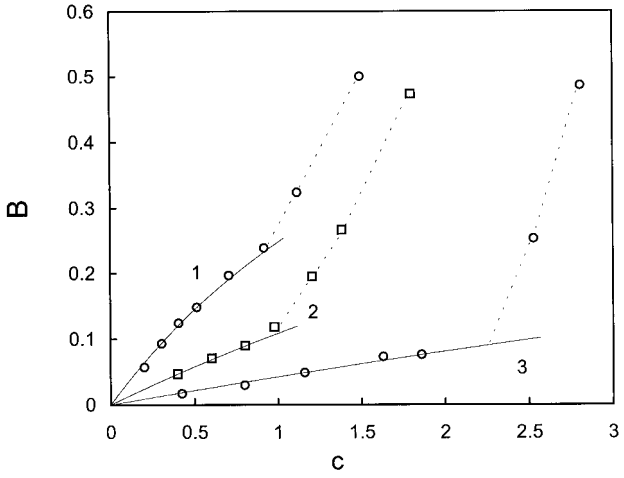

Figure 10 Dependence of the bound rubber fraction B on filler-to-polymer ratio c in SBR–carbon black compounds including the region of very high filler concentrations. Experimental points calculated from weighing data using eq. (8). Theoretical curves drawn using eq. (1b); parameter values given in Table III and the GPC molar mass distribution data. Dependences: 1—FEF, 2—lamp black, 3—MT black.

where D_1 is the number of reacted sites per unit of filler surface area during the first step, and D is the total number of reacted sites per unit of filler surface area in the finished compound. If β_1 is much smaller than β_2, then D_r ($= D_1/D$) should be small for a given D if one wants to have a high particle connectivity f. This could be an explanation for the behavior of graphitized carbon blacks: slow adsorption during the first step (i.e., small or zero D_r) leads to increased $(1 - D_r)$ and to a high f, in spite of the fact that graphitization results in a decreased value of D.

Surface modification of fume silica leads to a large decrease of D without significantly affecting the f-value. In this case the decrease of D was probably just compensated by the effect of increased $(1 - D_r)$.

Hot mixing probably leads to a rapid adsorption during the first step (high D_r) and the resulting f tends to be smaller than the f-value of the cold mixed compounds.

B in the Region of Very High Filler Concentration

Figure 10 shows the B vs. c dependence for three SBR–carbon black systems prepared using the mixing method A. In the region of very high filler concentration ($c > 1$ for FEF and lamp black, $c > 2$ for MT black) the experimental values of B

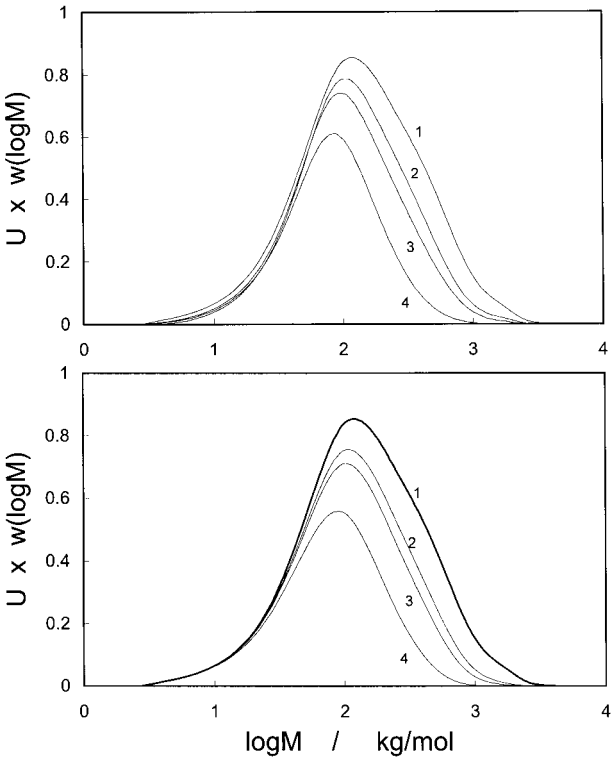

Figure 11 Top: curve 1—experimental molar mass distribution of SBR (5 min cold milled, $c = 0$). Curves 2, 3, and 4—experimental molar mass distributions of free (filler unbound) polymer multiplied by the respective U-values in the SBR–lamp black system; filler concentrations 1.2, 1.4, and 1.8, respectively. Bottom: curve 1—experimental molar mass distribution of SBR (5 min cold milled, GPC). Curves 2, 3, and 4—molar mass distributions (multiplied with U) calculated from curve 1 using eq. (12), ref. 4, and values of U and D given in Table V.

tend to increase more rapidly than would correspond to extrapolation from the region of low and medium values of c. A similar behavior can be seen for the SBR–ENSACO E50 system in Figure 5 (for high c, $B = G$). The observed effect is probably due to the mechanism proposed by Gessler.[9] Large shear stresses evolved during mixing may result in a breakdown of filler aggregates and/or formation of macroradicals through chain scission. Increased adsorptivity of freshly built filler surface and stabilization of polymeric macroradicals by grafting onto the carbon black surface would both lead to increased bound rubber formation. Very high shear stresses may be expected to develop during mixing in systems where the content of polymer does not suffice to fill the empty space between the filler particles (aggregates). This occurs at filler concentrations $c > c_{crit}$, where the critical concentration c_{crit} should be related to the reciprocal of DBPA or crushed DBPA (DBP 24M4). For MT black (DBPA < 40) the c_{crit} value can be expected to be high (neglecting the density difference between dibutyl phthalate and the polymer, $c_{crit} \approx 100/40 = 2.5 = 250$ mass parts of filler per hundred mass parts of polymer, phr), for carbon blacks with DBPA or DBP 24M4 around 100 the c_{crit} value would be ca. 1, i.e., about 100 phr.

Molar Mass Distribution of Filler-Unbound Polymer

Predictions of the statistical theory of bound rubber regarding the preferential adsorption of longer polymer chains were tested experimentally in our previous articles[3,4] using published data. Figure 11 (top) shows our own molar mass distribution curves of the filler-unbound polymer that was extracted from the compounds of SBR containing different concentrations of lamp black. Curve 1 is the normalized GPC molar mass distribution of SBR (5 min cold milled). Curves 2, 3, and 4 give the products of the respective normalized experimental molar mass distributions and of the respective experimental U-values. $U = 1 - B$ is the fraction of free (filler-unbound) polymer. The values of c and U are given in Table V, together with the D-values that were obtained from the experimental values of B and from the experimental molar mass distribution of SBR using eq. (7) of Part I. In Figure 11 at the bottom the experimental molar mass distribution of SBR (curve 1) is given once more while curves 2, 3, and 4 were calculated from it using eq. (12) of ref. 4. There are some small inconsistencies in the experimental distributions: the content of low-molar mass chains in free rubber extracted from filled compounds seems to be slightly smaller than that in the original polymer. Apart from this, the general agreement of the measured and calcu-

Table V Dependence of U, D, on c in the SBR-Lamp Black System

c	U	D (m^{-2}) $\times 10^{-16}$
0	1	
1.2	0.805	2.65
1.4	0.724	3.49
1.8	0.527	6.83

For $c < 0.9$, $D = 1.57 \times 10^{16}$ m^{-2}.

lated distribution curves is good. It should be noted that the compounds contain very high concentrations of lamp black, and the adsorption mechanism of the polymer on the filler, which is characteristic for the low and medium-c region, is obviously combined here with other mechanisms, probably with chemisorptive interactions of the Gessler type. The latter are expected to lead to a higher than normal yield of adsorbed polymer (higher D). Nevertheless, the changes of molar mass distribution of the free polymer with increasing bound rubber fraction still conform to the predictions of the PFGF theory (or, statistical theory of bound rubber). This suggests that even in the region of very high filler concentration the bound ruber formation still proceeds as a statistically random process.

CONCLUSIONS

The main conclusion of Part I was that the polymer–filler gel formation theory was able to describe, with a good success, experimental data obtained on compounds of NR and SBR containing fume silica. Results of Part II now show that the PFGF theory offers an equally good description of data obtained on compounds of SBR containing surface-modified (hydrophobized) fume silica and a number of carbon blacks differing in specific surface area and structure, both ungraphitized and graphitized. The values of the adjustable parameters D (filler surface adsorptivity) and f (functionality of crosslinks, measure of particles connectivity) were determined mostly by fitting theoretical curves to the experimental concentration dependences of the amount of polymer–filler gel.

D appears to be a good measure of specific filler surface activity for bound rubber formation, and unlike the quantity $B/c_{\mathrm{coh}}P$, it does not depend on polymer molar mass. D is surprisingly insensitive to the specific surface area of carbon black, tends to be higher for high-structure blacks, is significantly reduced by graphitization of carbon blacks, by hydrophobization of fume silica, and depends on mixing conditions, higher D being obtained at higher temperatures. In the region of very high concentration of carbon blacks, D was observed to increase significantly. This behavior was ascribed to the Gessler mechanism.

Most f-values lie in the range between 20 and 45; only graphitized blacks had larger values of f around 100. Again, f is rather insensitive to specific surface area of carbon black and depends on mixing conditions, higher mixing temperature, and higher shear stress having a tendency to give lower f-values. A qualitative explanation was proposed for the observed effects. With simplifying assumptions a theoretical value of f was estimated for a graphitized N330 carbon black aggregate and found to be several times larger than the measured f. Multiple segment adsorption of the same polymer chain on the same filler particle (i.e., closed loop formation) is proposed to be responsible for this behavior.

Molar mass distribution of filler-unbound polymer changes with the fraction of bound rubber in the manner predicted by the statistical theory of bound rubber even in the region of very high concentration of lamp black. Thus, polymer–filler interactions leading to bound rubber formation seem to proceed in a statistically random manner even in the presence of the Gessler mechanism.

The authors wish to express their thanks to the Grant Agency of the Czech Republic for the support of the work within the project No. 203/94/0915. Thanks are also expressed to Dr. Freund (Degussa AG) for providing us with a sample of graphitized carbon black N330 and to Mr.Smets (M.M.M. Carbon, Willebroek, Belgium) for providing us with a sample of ENSACO 50 E.

LIST OF SYMBOLS

c	concentration of filler, filler-to-polymer mass ratio
f	filler functionality
m	mass (kg); m_p mass of polymer, m_f mass of filler, m_{p1} mass of filler-unbound polymer, m_{p2} mass of polymer adsorbed on solvent-dispersed filler particles, m_{p3} mass of polymer in the polymer–filler gel, m_{f1} mass of solvent-dispersed filler particles, m_{f3} mass of filler in the polymer–filler gel
q	fraction of adsorbed polymer segments, q_{cr} fraction of crosslinked polymer segments
V_p	surface area of a filler particle (aggregate) (m^2)
$w(y)dy$	mass fraction of polymer chains having y in the range between y and $y+dy$
$w(\log M)$ $d \log M$	mass fraction of polymer having molar mass in the range between $\log M$ and $\log M + d \log M$

w_{disp} mass fraction of solvent-dispersed filler
y number of structural units (segments) in a polymer chain
A_o filler surface area per one active site (m^2)
B fraction of polymer adsorbed on filler, filler-bound polymer, bound rubber
CTAB cetyltrimethyl ammonium bromide
D number of active sites per unit of filler surface area (m^{-2})
DBPA dibutyl phthalate absorption (mL/g)
DBPA 24M4 dibutyl phtalate absorption measured on a preliminary compressed filler
G fraction of gel polymer
M molar mass of polymer (kg/mol), $\overline{M}_n$ number average, $\overline{M}_w$ mass average, $\overline{M}_z$ z-average, $\overline{M}_v$ viscosity-average, M_o molar mass of a polymer segment (structural unit), M_r relative molecular mass
N_A Avogadro constant, 6.023×10^{23} mol^{-1}
P specific surface area of filler (m^2/g), P(CTAB) specific surface area determined using CTAB adsorption
R mass ratio, R_p mass of polymer–filler gel per unit mass of polymer, R_f mass of polymer–filler gel per unit mass of filler, R_3 polymer–filler mass ratio in the gel, R_{f3} mass of polymer–filler gel per unit mass of filler in the gel
β fraction of those adsorbed polymer segments that conform to the requirement of no loop formation
γ crosslinking index, number of crosslinked units per mass-average macromolecule
$[\eta]$ limiting viscosity number (dL/g)

REFERENCES

1. L. Karásek and B. Meissner, *J. Appl. Polym. Sci.,* **52,** 1925 (1994).
2. B. Meissner, *Theory of Polymer–Filler Gel,* Prague Microsymp. Macromol.14th IUPAC, Prague, 1974; B. Meissner, *Sci. Pap. Prague, Inst. Chem. Technol.,* **S3,** 223 (1980).
3. B. Meissner, *J. Appl. Polym. Sci.,* **18,** 2483 (1974); *Rubber Chem. Technol.,* **48,** 810 (1975).
4. B. Meissner, *J. Appl. Polym. Sci.,* **50,** 285 (1993).
5. B. Meissner, *Rubber Chem. Technol.,* **68,** 297 (1995).
6. W. C. Carter, R. L. Scott, and M. Magat, *J. Am. Chem. Soc.,* **68,** 1480 (1946).
7. T. Homma and J. Fujita, *J. Appl. Polym. Sci.,* **9,** 1701 (1965).
8. S. Wolff, M.-J. Wang, and E.-H. Tan, *Rubber Chem. Technol.,* **66,** 163 (1993).
9. A. M. Gessler, Rubber Chem. Technol., **42,** 858 (1969).
10. B. Meissner and L. Karásek, *Polymer,* to appear.